THE JOURNAL OF PHYSICAL CHEMISTRY B

ARTICLE

pubs.acs.org/JPCB

Charge-Induced Conformational Changes of PEG-$(Na^+)_n$ in a Vacuum and Aqueous Nanodroplets

Styliani Consta* and Jun Kyung Chung

Department of Chemistry, The University of Western Ontario, London, Ontario, Canada N6A 5B7

ABSTRACT: Charged-induced conformational changes of sodiated poly(ethylene glycol) (PEG-$(Na^+)_n$) in a vacuum and water droplets were studied using molecular simulations. In a vacuum, compact and partially unwound conformations were identified by analyzing occupation probabilities on reaction surfaces defined by the accessible surface area of the macroion, the distance between the centers of mass of the PEG molecule and of the cations and radius of gyration of the macromolecule. The critical charge of the macromolecule for which there is coexistence of various conformations was estimated using the Rayleigh criterion for the breakdown of highly charged droplets and compared with that observed in the simulations. The simulation findings agreed well with the Rayleigh prediction. The properties of sodiated PEG macromolecules in the presence of solvent and ions were also investigated. It was found that the macroion becomes saturated with charge. The highly charged state leads to an extended conformation that is partially expelled by the droplet. However, a portion of the chain is still in contact with the solvent. Drying-out of the solvent leaves the macroion in a stretched necklace-like conformation. The mechanism of release of sodiated PEG from an aqueous droplet was shown to be distinctly different from that of a protonated polyhistidine in a water nanodroplet, demonstrating sensitivity of the disintegration mechanism of the nanodroplet to the degree of hydrophilicity of the macroion.

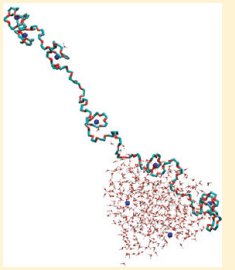

INTRODUCTION

Charge-induced conformational change of macromolecules is an important process in biological macromolecules such as DNA and proteins. For instance, proteins may change conformations or denature depending on the pH value of the solution. Understanding dependence of the conformation of a macromolecule on its charge is also a central issue in the choice of optimal experimental conditions and interpretation of data in electrospray mass spectrometry (ESMS) experiments.[1−11] In electrospray (ES), a macromolecule is transferred from the bulk solution into the gaseous state via droplets that carry ions and solvent in addition to the macroion. In the last twenty years, several questions have been posed concerning the relation of the droplet charge with conformation of macroions in the droplets and vacuum. In this article we will focus on two of those questions: (i) charge-induced conformational changes of PEG macroions in a vacuum; (ii) solvation and release of PEG macroions from droplets. These questions are investigated by molecular simulations of sodiated-PEG in a vacuum and water droplets. Simulations of conformational changes of PEG-$(Na^+)_n$ in a vacuum provide us with reference ranges of charge versus degree of polymerization of PEG that are useful in understanding the behavior of PEG-$(Na^+)_n$ in droplets. Even though aspects of the former question have been explored by many experimental, computational, and theoretical studies of related problems, molecular simulations of sodiated PEG have not been reported so far. In experiments Hudgins et al.[12] observed unfolding of cytochrome C induced by changing its charge state. Mao et al.[3] conducted computational study of corresponding system and obtained qualitative agreement between molecular dynamics simulations and experimental data. Ude et al.[13] used ammoniated poly(ethylene glycol) chains of various lengths and charge states and found that for low charge states, the molecules assume near spherical shape and at some critical charges, abrupt unfolding happen. In theory, valuable insight into charged-induced conformational changes of macromolecules in a vacuum has been obtained by Burin et al. who employed Flory's mean field theory and lattice models.[14] The study of a single polymer with external charges showed that strong short-range interactions relative to electrostatic give rise to a discontinuous jump in radius of gyration (R_{gyr}) at a critical amount of charge. The transition is first-order and the coexistence of compact-extended conformations was described by a bistable free energy profile along R_{gyr}. Because of the assumptions of the underlying theory, the study leaves open the question of the morphology of the various conformations of the chains. Furthermore, the analysis is based on the radius of gyration of the system that may not be an appropriate reaction coordinate to clearly distinguish two states and reveal the transition mechanism. On the simulation side, Tapia et al.[15−17] conducted extensive simulations of lysozyme ions in a vacuum and found coexistence of compact and non-compact structures for a range of charge values. In those studies folding−unfolding transitions were observed by starting from an ensemble of configurations in one state and inducing the transition. In this paper, our goal is to examine the various aspects addressed separately by previous works in a unified way that uses a realistic model. Sodiated PEG was simulated because it has been a broadly used experimental model[1,2,13,18] and also provides

Received: May 16, 2011
Revised: August 3, 2011
Published: August 03, 2011

dx.doi.org/10.1021/jp204559y | J. Phys. Chem. B 2011, 115, 10447–10455

a reasonable compromise between reality and simplicity of molecular interactions. We determine the critical charge that allows for a reversible transition between compact to extended state for sodiated PEG in a vacuum and examine whether Rayleigh's model can predict the critical charge. We find that Rayleigh's criterion of instability for a charged droplet,[19] when applied to charged polymer, gives estimate of the critical charge substantially close to that predicted by simulations. This was first argued by Ude et al.[13] using their ion mobility spectrometry data of ammoniated PEGs. To our best knowledge, related computational study to the experiment has not been reported as yet. Next, we take a close look at the mechanism of the transition by simulating PEG−sodium ion systems that have charges close to critical ones. Using a combination of reaction coordinates for PEG with up to approximately 100 monomers we find the coexistence of two states, which is consistent with previous theoretical and computational works.[14,17] For PEG with 150 monomers charged with five Na^+, three states are identified to coexist. We find that the mechanism of polymer destabilization is close to the ion-evaporation mechanism (IEM).[20−23] In the same fashion as in IEM for charged droplets with simple ions,[22,23] moderately below the critical charge, the chain may become partially unwound. In the course of unwinding, a single Na^+ coordinated by oxygen sites of PEG escapes from the compact part of sodiated PEG overcoming a free energy barrier.

Next, the charged PEG is solvated and its conformations are monitored as the droplet disintegrates. Study of the conformational changes and finally the drying-out process is central in understanding the macroion release mechanism from a droplet. Escape mechanism of ions from charged droplets have been discussed in the seminal works of Dole[24] who developed the charge residue model (CRM) and Fenn[25] who generalized the ion-evaporation model (IEM)[20,21] for macroions. The question about what escape mechanism is typical in an experiment has been a topic of long-standing debate in the literature.[7,10,26,27] To our knowledge the conformational changes of charged PEG in a droplet and the subsequent release mechanism have not been studied in silico so far. It is found that PEG-$(Na^+)_n$ in charged aqueous nanodroplets becomes saturated with charge and attains a stretched conformation. The location of the charged PEG on the surface of the droplet facilitates partial extension outside the droplet, while a portion remains solvated. Drying-out of the solvent leaves the macroion in a necklace-like stretched conformation. Comparison with our previous studies on charged polyhistidine in water nanodroplets,[11] exhibits that the manner that the macroion emerges from the droplet is sensitive to the degree of its hydrophilicity.

MODEL AND COMPUTATIONAL METHODS

Computer modeling of PEG in a vacuum and aqueous nanodroplets was carried out using DL_POLY[28−30] molecular simulation program. The PEG molecules were modeled by the OPLS united atom force field.[31] A variety of lengths of PEG molecules in the range of 32−256 monomers were simulated. The length of PEG will be indicated hereafter as PEG*N*, where *N* is the number of monomers. Nonbonded interaction parameters for sodium ions were taken from ref 32. Water molecules were represented by the flexible SPC.[33] No distance cutoffs were imposed on the forces within the systems.

PEG-$(Na^+)_n$ in a Vacuum. Initial configurations of the sodium saturated PEG molecules were created using MD and subsequent annealing in a system without electrostatic interactions. The resulting compact conformation was used as a seed for the study. For PEG molecules up to 96 monomers, MD simulations in canonical ensemble with Nosé−Hoover thermostat[34,35] were performed at T = 300 K. The time step of the simulations was 1 fs. Direct simulations were performed up to 600 ns. For PEG molecules with length of 100 or more, the parallel tempering[36−38] method was implemented together with hybrid Monte Carlo (HMC) scheme[39,40] to facilitate sampling of various sodium ion configurations. In the parallel tempering or replica exchange method several copies of the system are simulated simultaneously at different temperatures. Additional Monte Carlo (MC) involving exchange of conformations at different temperatures was used to enhance sampling. The acceptance probability for the exchange MC is given by

$$\min\{1,\exp[(\beta_i - \beta_j)(U_i - U_j)]\} \quad (1)$$

where $\beta_i = (k_B T_i)^{-1}$ is the inverse temperature for the ensemble at temperature T_i, U_i is the potential energy, and k_B is the Boltzmann constant. For PEG150, canonical ensembles at 300, 314, 329 , 344, and 360 K were simulated. The temperatures were chosen experimentally to yield average acceptance probability (1) close to empirical optimal value 1/3. HMC moves were accomplished by running a short trajectory using the velocity Verlet algorithm with the initial velocities assigned from Maxwell−Boltzmann distribution. The length of the trajectory was taken to be 0.2 ps and the time step 2 fs. One Monte Carlo step (MCS) consisted of 10 HMC moves and 1 move to exchange configurations between randomly selected two adjacent ensembles. For PEG150, 5×10^5 MCS were performed. The parallel tempering method was implemented by modifying existing DL_POLY code.

To monitor conformational changes, occupation probability surfaces were estimated vs two reaction coordinates: (i) the accessible surface area and the distance between the centers of mass of PEG and sodium ions and (ii) the distance between the centers of mass of PEG and sodium ions and the radius of gyration.

PEG-$(Na^+)_n$ in Water. A system of PEG96-$(Na^+)_4$ in a droplet of 800 water molecules was simulated by Nosé−Hoover MD at 300 K. The runs were for 20 ns. Initial configurations were prepared by placing a shell of 800 water molecules around a compact conformation of PEG96-$(Na^+)_4$ taken from vacuum simulations. Simulations were also performed for PEG96-$(Na^+)_4$ in 800 water molecules with six Na^+. The simulations were performed at 300 and 350 K. The electrostatic potential on the surface of the droplet was analyzed.

RESULTS AND DISCUSSION

Distribution of Ions along PEG-$(Na^+)_n$. An important issue in simulating the PEG−sodium ion systems is adequate sampling of the various locations of the ions, which may require extremely long simulations. To examine the mobility of ions, the positions of the ions of PEG150 and PEG96 were monitored for hundreds of nanoseconds. The position of a sodium ion along a PEG chain is defined as a weighted average of indices of monomers around the ion. The weighting factor is chosen to be inversely

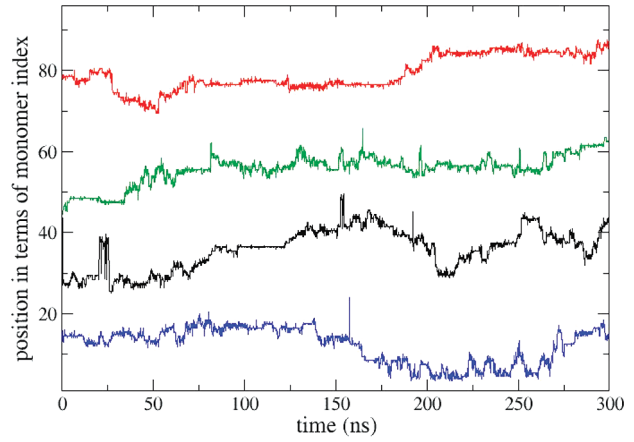

Figure 1. Positions of four Na^+ ions along the PEG96 measured in terms of the monomer index using direct MD.

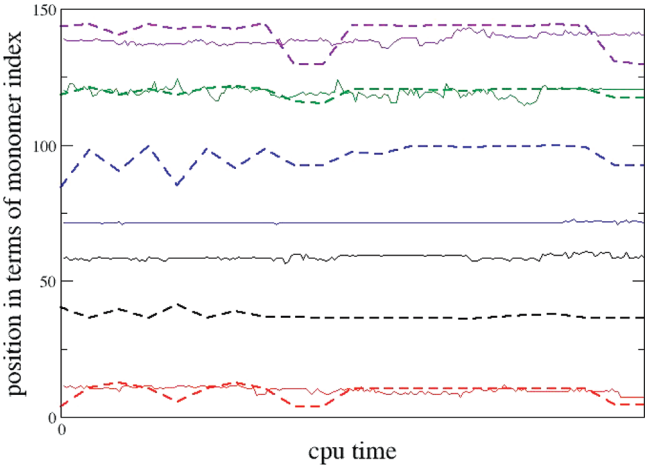

Figure 2. Positions of five Na^+ ions along the PEG150 measured in terms of the monomer index. Dashed lines are obtained from parallel tempering Monte Carlo simulations and solid lines are obtained from 20 ns NVT MD simulations.

proportional to the distance between the ion and the oxygen site of a monomer, i.e.,

$$S_i = \frac{1}{A_i} \sum_{j=n_1}^{n_k} \frac{I(j)}{r_{ij}} \qquad (2)$$

where n_1, ..., n_k are indices of oxygen sites within 3 Å of the sodium ion labeled i, $I(j)$ is the monomer index to which oxygen j belongs, r_{ij} is the distance between sodium i and oxygen j, and $A_i = \sum_{j=n_1}^{n_k} 1/r_{ij}$ is the normalization constant. The number of neighbors of a sodium ion k was found to be typically between 4 and 7.

Figure 1 shows the positions of ions as function of time for PEG96-$(Na^+)_4$ (for the choice of the numbers of ions, see next section). The ions maintain their relative locations with respect to each other while they can explore locations in the chain by up to 20 monomers over 300 ns. The ions of PEG96 have higher mobility compared to those of PEG150.

To facilitate sampling of ion configurations, parallel tempering method was implemented for a PEG150-$(Na^+)_5$. In Figure 2, the mobilities of sodium ions from *NVT* MD and parallel tempering

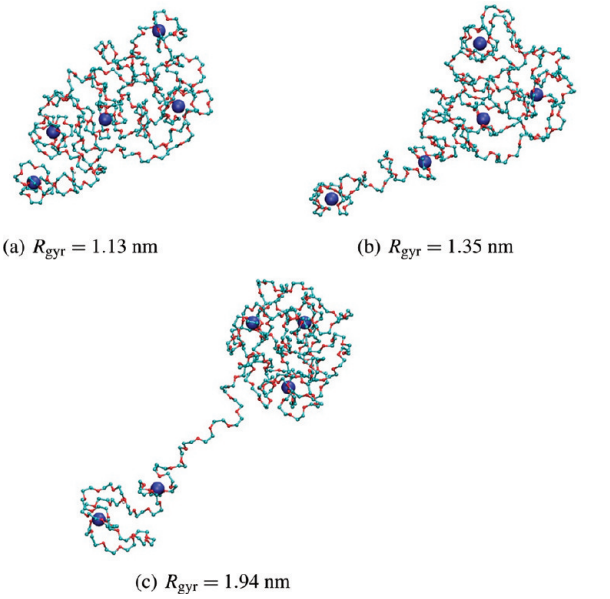

Figure 3. Typical conformations of PEG150-$(Na^+)_5$ in compact (a), transition (b) and extended states (c). In the direct MD simulations multiple transitions between states have been observed.

Monte Carlo are compared. It is clearly seen that the latter method samples the ion's positions more efficiently than regular MD. The compact-extended chain transitions in studied systems take place on much shorter time scale than the transfer of sodium ions along the polymer chain as illustrated in Figures 1 and 2. Due to aforementioned time-scale separation between the two processes the reported results depend on the preparation of the system and correspond to properties of metastable rather than equilibrium ensemble. Nevertheless, simulations of systems starting from varying initial condition resulted in consistent picture of the compact-extended chain transformations. As will be discussed later, parallel tempering method was able to sample extended conformations of the PEG150-$(Na^+)_5$, while *NVT* MD was not.

Characterization of the Conformational Changes of PEG-$(Na^+)_n$. Typical conformational changes of PEG150-$(Na^+)_5$ with corresponding values of R_{gyr} are shown in Figure 3. The way the charge is chosen is discussed in the following section. As seen in Figure 3, extended conformations are often partially unwound; thus, hereafter the term "extended" will be used to mean partially unwound as well as fully open conformations.

Increase in the system charge affects conformational changes of the PEG molecule. Conceptually, it is incorrect to associate a specific conformation as a typical representative of a charged PEG macromolecule. Rather a system with any given charge samples an extensive array of conformations spanning very distinct areas of the conformational space: the globular state and the extended state. The charge of the system changes not the preferred conformation but rather the relative populations of various samples. We contrast this picture with globule−coil transition in homopolymers.[41,42] The transition from globule to coil for finite length chains takes place at around θ temperature with continuously increasing order parameter, typically the radius of gyration. In the case of the charge induced globule-extended transition the observed picture is manifestly different. At the critical charge the PEG molecule populates both globule and extended states that are in dynamic equilibrium.

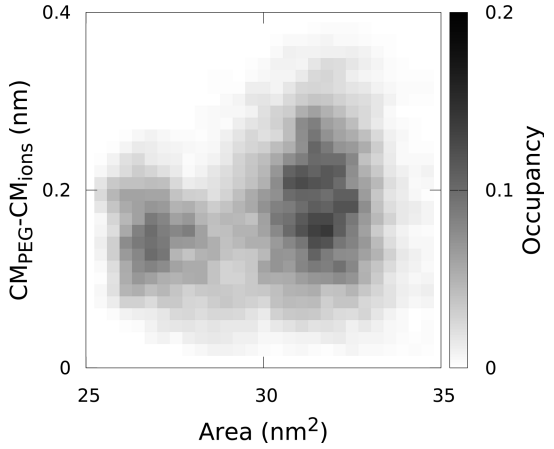

Figure 4. Occupation density profile on the reaction surface of the PEG96 macromolecule in the presence of four sodium ions. The reaction surface is parametrized by accessible surface area (horizontal axis) and the distance between ions and PEG centers of mass (vertical axis). Two high-occupancy states can be distinguished in the plot. The surface area of compact conformations typically does not exceed 29 nm^2 and, in the case of extended conformations, the surface is larger than 29 nm^2.

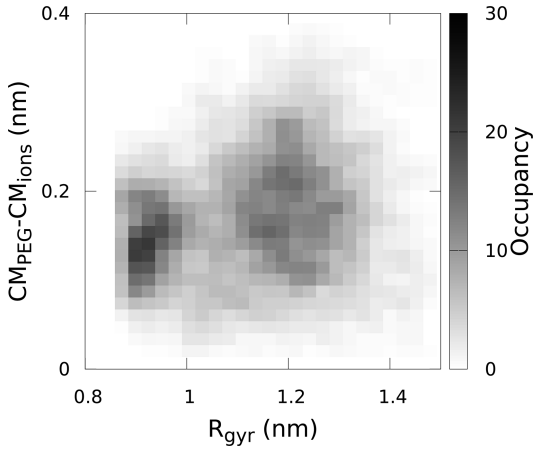

Figure 5. Occupation density profile on the reaction surface of the PEG96 macromolecule in the presence of four sodium ions parametrized by the radius of gyration of the PEG molecule. The vertical axis is the distance between ions and PEG centers of mass. The compact and extended states are readily identified. A separatrix between two states is not well approximated by a line R_{gyr} = const making the single reaction coordinate R_{gyr} unsuitable for description of the transitions between states.

We illustrate this behavior in Figures 4 and 5. A PEG96 molecule saturated with four sodium ions is close to the critical transition. Occupational densities of PEG96 conformations are shown as histograms of populations on reaction coordinate surfaces. In Figure 4 the reaction surface is defined by the polymer accessible surface area (ASA) and the distance between centers of mass of ions and the polymer. In Figure 5 we use the polymer radius of gyration instead of ASA. The distance between centers of mass of ions and the polymer is chosen as the second reaction coordinate to discriminate between systems with uniformly solvated ions and the rest.

In Figure 4 the histogram shows the presence of two distinct states: globular and extended. The difference in ASA between

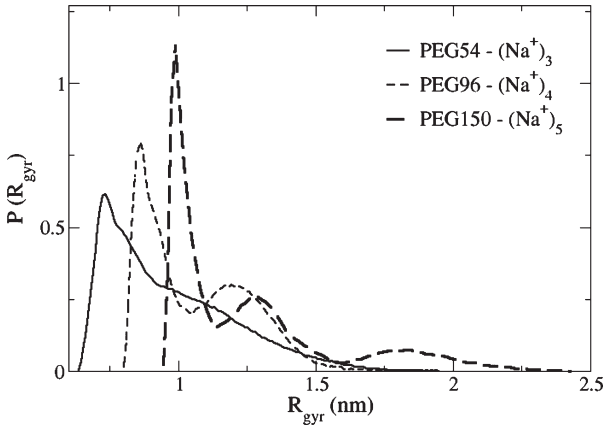

Figure 6. Probability density of R_{gyr} for simulated PEG-$(Na^+)_n$ with n = 3−5.

extended and compact states is 6 nm^2. The corresponding fraction of monomer units in the secondary droplet $[x]$ is estimated through dimension analysis using the following equation for the total surface area:

$$(1 - [x])^{2/3} + [x]^{2/3} = \frac{\mathrm{ASA}_{\mathrm{extended}}}{\mathrm{ASA}_{\mathrm{globule}}} \quad (3)$$

Computations yield for the fraction of monomers in the secondary droplet value $[x]$ = 0.16. This corresponds to approximately 15 monomer units in PEG chain of length 96. This value agree with experimental observations (Figure 3).

In Figure 5 the histogram was built using R_{gyr} as one of the reaction axes. The presence of two states is less obvious than in the case of ASA as the other reaction coordinate. While both reaction coordinates monitor the same kind of changes, the radius of gyration is inferior. From the occupation densities plots it is also clear that the use of only one reaction coordinate, either the ASA or the radius of gyration, is problematic. The valley separating the two states is not parallel to the other axis, lowering the height of the barrier corresponding to the transition state (Figure 6). A more comprehensive search for proper description of the expansion mechanism is required to determine the best reaction coordinate characterizing globule-extended transition.

Even though R_{gyr} is insufficient to show reliably the relative stability of compact-extended states and the transition state, it can still be used to indicate the existence of important conformations. Figure 6 shows different behaviors of PEG54-$(Na^+)_3$, PEG96-$(Na^+)_4$, and PEG150-$(Na^+)_5$. PEG54-$(Na^+)_3$ undergoes frequent transitions between compact and extended conformations. The extended conformation observed does not correspond to a local maximum in probability density profile (PDP). Due to the small size of the system, the distribution of R_{gyr} values are wide, allowing the molecule to extend and contract without having to cross a substantial free energy barrier. Differently from the smallest PEG54-$(Na^+)_3$, PEG96-$(Na^+)_4$ does develop two local maxima in its PDP, as shown in Figure 6. PEG150-$(Na^+)_5$ shows three states where one (Figure 3b) and later two Na^+ ions (Figure 3c) encaged by the oxygen sites of PEG escape. In the three lengths of chain the first maximum corresponds to compact conformations, as shown in Figure 3a. Calculations of the average potential for conformations of PEG54-$(Na^+)_3$, PEG96-$(Na^+)_4$, and PEG150-$(Na^+)_5$ characterized by R_{gyr} showed that the compact conformations are energetically

favorable, and as the PEG extends, the average potential energy increases. The free energy (F) is written in terms of the probability ($P(R_{gyr})$) of finding a configuration with a specific value of R_{gyr} is $F = -k_B T \ln P/P_0$, where P_0 is the uniform density of R_{gyr}. The entropic contribution that was estimated by subtracting the average potential energy from F shows that the shaping of the free energy profile with a barrier is attributed to the entropic term ($T\Delta S$) of the free energy.

The overall picture that emerges from our simulations is that for a narrow range in the ratio of the square of charge to length of PEG, various conformational states can coexist. For PEG96-$(Na^+)_4$, direct MD runs showed the rate of transformation 0.015 ns^{-1} between distinct conformations characterized by R_{gyr}, while several intermediate conformations survive for approximately 1 ns. The connectivity of the polymer precludes the existence of an unbound state once it partially unwinds. This mechanism of destabilization is distinctly different from a liquid charged droplet, where below the critical charge a solvated ion can escape by overcoming a free energy barrier without possibly reconnecting to the remaining of the droplet. Even though the mechanism of release of charge in droplets is different from that in polymers, in the following section we show that the Rayleigh model for the critical charge of a droplet, provides an excellent prediction for polymers as well.

Estimate of the Critical Charge. The transition from compact to extended conformations is "first-order-like" in the sense that R_{gyr} as a function of total charge shows a discontinuous jump.[14] Therefore, we adopt the definition of critical value used in the context of first-order phase transition. That is, the critical charge for a given PEG is defined in such a way that the free energy as a function of R_{gyr} has two local minima corresponding to the same value of free energy.[43,44] In practice, however, it would be hard to pinpoint this amount of charge and one would have to introduce a fractional number of sodium ions. To avoid these unrealistic systems, initially, we identify upper and lower bounds of the unknown critical charges for PEG-$(Na^+)_n$ of various lengths. A lower bound is defined by the amount of charge that will make a given PEG assume a compact conformation at its equilibrium state (e.g., Figure 3). Several initial conformations were tested to confirm that the compact state is the prevalent conformation for the system. In the test runs the number of sodium ions that were placed approximately evenly along the chain were varied and MD simulations for at least 20 ns for every system were performed to determine their approximate equilibrium configuration. In a similar way upper bounds to the critical charge were identified where the conformations are partially unwound (e.g., Figure 3b,c). Upper and lower bounds estimates for N = 32, 64, 128, 256 are shown in Figure 7.

As a guide to analysis of the obtained bounds, we use Rayleigh's criterion for the stability of charged conducting spherical droplet,[19] given by

$$Q_c^2 = 64\pi^2\sigma\varepsilon_0 R^3 \quad (4)$$

where Q_c is the critical amount of charge, σ is surface tension, and R is the radius of the droplet. The original Rayleigh model concerns charged droplets but does not specify the microscopic detail of the system. Considering monomers of a PEG molecule to be molecules that solvate sodium ions and using the relation $N \propto R_{gyr}^3$ for compact structures,[45] one obtains a scaling relation between the critical charge and the degree of polymerization

$$Q_c = c\sqrt{N} \quad (5)$$

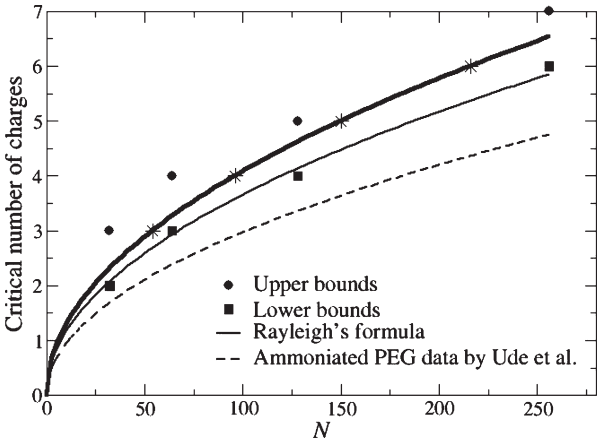

Figure 7. Estimation of critical charges. Circles and squares represent the upper and lower bounds to critical charge, respectively. The thick black line that scales as $(N/6.0)^{1/2}$ was used to estimate N corresponding to the integer value of the critical charge. The black thin line was obtained from Rayleigh's criterion using literature values of surface tension and density for PEG.[46] The black dashed line is obtained using data by Ude et al.[13]

with some unknown constant of proportionality c, which should be material dependent constant, but independent of N. Therefore, for our simulations it can be considered to be constant regardless of the degree of polymerization and we treat it as a fitting parameter in estimating critical charge.

On the other hand, to estimate the exponent of scaling relation independently of Rayleigh's model, one may assume a simple relation $Q_c \propto N^\alpha$ and fit upper and lower bounds separately. Fitting upper bounds yielded $\alpha \approx 0.52$, while the data for lower bounds gave $\alpha \approx 0.41$. From these procedures, we concluded that α must be between 0.41 and 0.52, which is still consistent with the prediction of Rayleigh's criterion.

In Figure 7 the thick black line represents (5) with c adjusted such that it stays within the upper and lower bounds points. From this curve, we estimated that the critical number of sodium ions for PEG54, PEG96, PEG150, and PEG216 would be close to 3−6, respectively. Although not exact, we expect that the estimation will provide systems close to critically charged PEG molecules, therefore exhibiting coexistence of both compact and extended conformations.

In the same figure, also shown is the line obtained by using (4) with PEG surface tension value taken from ref 46. The estimate represented by the black thick line in Figure 7 does not use the value of surface tension. In Figure 7 the experimental data for ammoniated PEG by Ude et al.[13] are also shown. The comparison of Rayleigh's prediction, simulation findings, and experimental data show approximately $Q_c \propto \sqrt{N}$ scaling behavior for the charged PEG systems in a vacuum.

PEG96-$(NA^+)_4$ IN NANODROPLETS OF WATER

In this section, we show that if a PEG molecule charged with sodium ions is placed in a droplet of water, its conformational behavior changes dramatically relative to the vacuum situation. On the basis of the critical value of charge predicted by Rayleigh, two regimes are studied, below and close to the Rayleigh limit. For the case below the Rayleigh limit, PEG96-$(Na^+)_4$ in 800 water molecules was simulated at 300 K. For the study close to the Rayleigh limit PEG96-$(Na^+)_4$ was placed in 800 water

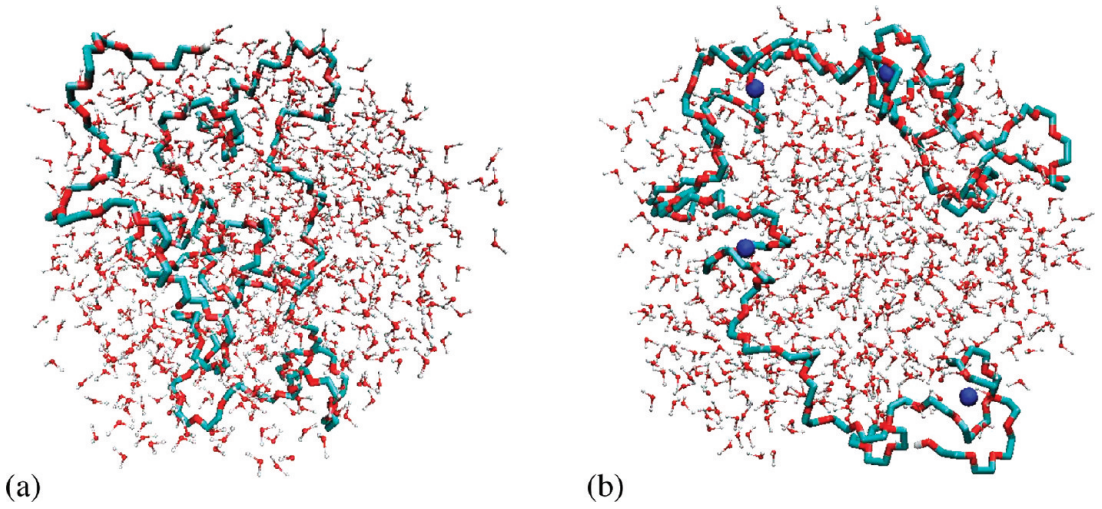

Figure 8. (a) Neutral PEG96 molecule in a droplet of 763 water molecules. The whole molecule prefers to stay in the interior of the droplet due to its hydrophilicity. (b) PEG96-$(Na^+)_4$ in a droplet of 713 water molecules after 5 ns *NVT* MD simulation.

molecules that contained four or five Na^+. The number of additional Na^+ was led by Rayleigh's prediction of critical charge of 10e for a droplet of 800 water molecules and a single PEG96. In the estimate it was assumed that the PEG96 and 800 water molecules are approximately equivalent to 1000 water molecules. The surface tension of water (71.97 mN/m) was used in the estimation. If the PEG surface tension (42.5 mN/m) is used, then the critical Rayleigh charge is 8e. After energy minimization of the configurations, *NVT* MD at 300 and 350 K with Nosé–Hoover thermostat were performed and conformation was monitored for at least 10 ns.

For comparison purposes, a neutral PEG96 in a droplet of 800 water molecules was prepared. Our simulations indicated that neutral PEG molecules assume compact conformations in a vacuum. When PEG96 was put in the droplet, however, we found that the conformation changes to an extended shape, where the most of PEG prefers to stay in the interior of the droplet, as shown in Figure 8a. This behavior is consistent with its known hydrophilicity.

Charge State of Nanodroplet below Rayleigh's Limit. Figure 8b shows a snapshot at the end of a 5 ns simulation. During all simulation times, the chain stays along an arc on the surface of the droplet. The average R_{gyr} of PEG96-$(Na^+)_4$ ($\approx$1.6 nm) is found to be slightly larger than that of neutral PEG96 ($\approx$1.3 nm). The tendency of PEG96-$(Na^+)_4$ to stay close to the surface of the droplet can be explained by the orientation of the hydrophilic oxygen sites and hydrophobic $-CH_2-$ sites. The Na^+ ions are coordinated by PEG oxygen sites, which increseases by a small amount the percentage of $-CH_2-$ exposed toward the interface with water. Even though several oxygen sites of PEG continue to interact directly with water, a small increase in the hydrophobic interactions expel PEG96-$(Na^+)_4$ on the surface. The charge alone cannot be the reason for the location of PEG96-$(Na^+)_4$ on the surface because the water molecules can reduce the repulsion between the charges by screening and redistribute the charge density on the surface of the droplet. This could result in a charged hydrophilic molecule solvated by water[11] in a similar way as the neutral PEG in water droplet. However, this is not the case in the present simulations because of changes in the orientation of $-CH_2-$ and PEG oxygen sites. During a 10 ns run, no transfer of Na^+ from PEG to water was observed. Even though in a vacuum PEG96-$(Na^+)_4$ undergoes compact-extended conformational changes, in the water nanodroplet we do not expect these transformations. A compact conformation is very unlikely to form because interactions of water and PEG have to reorganize considerably. It is noted that the expulsion of the charged macromolecule on the surface of the droplet is unique in finite-sized systems because in bulk water it is expected that the charged PEG will take a compact conformation with the hydrophobic sites exposed toward the solvent. Because it has been found that PEG96-$(Na^+)_4$ in a vacuum undergoes compact-extended transformations, the compact conformation that carries charge +4e is still a plausible conformation even in the bulk.

As will be discussed in the next section, the location of the macromolecule on the surface affects the charge that may hold and then how it finally emerges from the droplet.

Charge State of Nanodroplet Close to Rayleigh's Limit. When PEG96-$(Na^+)_4$ is placed in the droplet with four or five additional Na^+, it prefers to stay on the surface attaining an extended conformation with a slightly larger R_{gyr} than the neutral PEG. Over the course of 10 ns simulations, it was observed that two of the Na^+ initially found in water were transferred from water to PEG96-$(Na^+)_4$, as shown in Figure 9a, while the reverse motion was not observed. The point of the transfer of ions from the solvent to the PEG deserves consideration. The process is seemingly counterintuitive because the Na^+ would be more favorably solvated by the water oxygen sites with partial charge $-0.82e$ instead of the oxygen of PEG molecule with partial charge $-0.5e$. However, the system is quite complex and contains interfaces of water–vacuum, water–PEG, and PEG–vacuum as well as solvation of ions. The complexity of the interactions and at the same time the size of the system that may makes these interactions influence each other may lead to complex solvation phenomena that do not conform with the simple electrostatic picture of solvation of Na^+ by the oxygen sites of water or PEG. This is a possible reason for the transfer of Na^+ from water into PEG. The analysis of radial distribution functions of the hydrogen site of H_2O (HW)-CH_2, the oxygen site of H_2O (OW)-CH_2, HW-OPEG, and OW-OPEG in the interface of PEG and water did not show differences in the location and intensity of peaks between PEG96-$(Na^+)_4$ and PEG96-$(Na^+)_6$ in water. Even

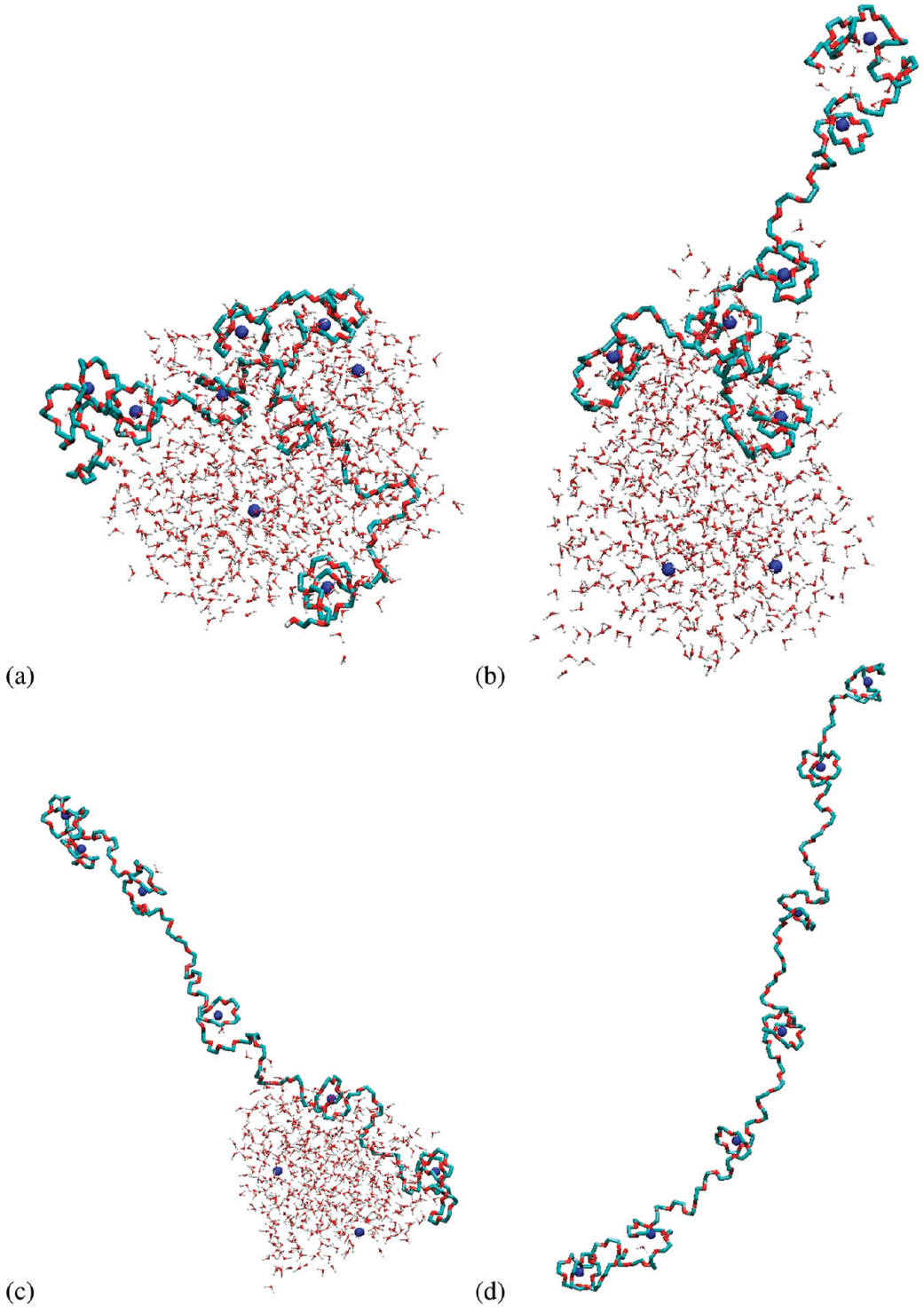

Figure 9. Snapshots from the simulation of PEG96-$(Na^+)_4$ in a droplet of water at $T = 350$ K with four additional ions distributed in the water. (a) Initial equilibrated configuration. The PEG has trapped six Na^+ where two Na^+ have transferred from the water. Approximate estimate of the radius of PEG96-$(Na^+)_6$ is 17 Å. Evolution of the system at (b) 0.75 ns, (c) 1.9 ns, and (d) 18 ns. The PEG has a total of seven Na^+ when all the water molecules evaporate.

though the energetic reason is plausible, it seems that fluctuations lead the Na^+ toward PEG as they lead them to escape from other locations on the surface of the droplet. Once the Na^+ enter the PEG region, they are trapped by the oxygen sites that form a rigid structure around them. Because PEG lies in the water−vacuum interface, once it obtains charge beyond its Rayleigh critical charge, it attains the vacuum conformation that corresponds to this amount of charge and becomes extended. Part of the chain extends out of the chain, while a part is still solvated (Figure 9b,c). Finally, as shown in Figure 9d all the water evaporates and the PEG96-$(Na^+)_n$ is left charged by 7 Na^+. The process described was reproduced using a few different initial configurations at 300 and

dx.doi.org/10.1021/jp204559y |*J. Phys. Chem. B* 2011, 115, 10447–10455

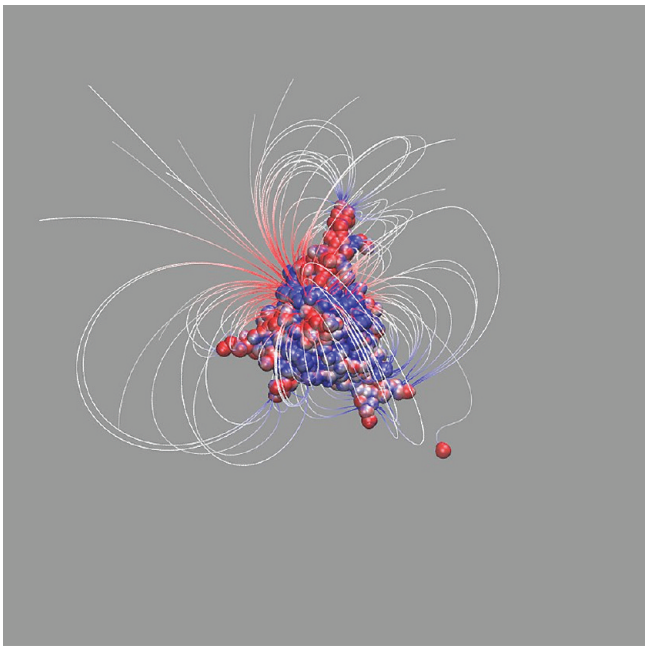

Figure 10. Electrostatic potential on the vdW surface of the droplet and field lines of the electrostatic potential of the system with excluded sodium ions. The electrostatic potential is mapped on the vdW surface of the droplet. The values of the potential in units of unit charge over Å are shown using red-white-blue color-map. The values of the potential range from 0.45 Z/Å (red) to 0.55 Z/Å (blue) (see text).

350 K. As expected, the dynamics of the process depends strongly on the temperature, at 300 K the process lasts an order of magnitude longer than at 350 K shown in Figure 9. Realizations were also performed for a droplet of the same size as the reported data for 350 K but with overall charge 10e. It is observed that the system is found in the instability regime, because initially the solvent forms spines, and then the sodiated PEG escapes in a similar manner as when the charge is slightly below the critical value.

To examine further the charge distribution on the surface, the electrostatic field around the droplet was estimated. Figure 10 shows the electrostatic field around a droplet composed of 760 water molecules, PEG54 and 10 sodium ions. Rayleigh's model predictions are based on the assumption of existence of mobile charges and, as a consequence, uniform electrostatic potential on the surface of the droplet. In the presence of PEG macromolecule this assumption breaks down in the course of spherical droplet evolution. The main reason for this is the strong noncovalent bonding of the PEG molecule and sodium ions and reduced mobility of the charges. Nevertheless, the variations in the potential 0.45−0.55 Z/Å are orders of magnitude smaller than the corresponding variance of a potential induced by a point charge +10 Z on the equivalent surface. The field lines show polarization of the solvent due to distribution of the sodium ions. The field lines of the solvent induced electrostatic field show charge transfer by the polar solvent from the central region (position of the solvated PEG54) to the tips of the spines. The development of the observed spines in supercritical droplets is a common theme in the evolution of instabilities in charged systems.[11]

The manner that PEG96-$(Na^+)_n$ emerges from the droplet is different from the mechanism that was found for a multiply charged polyhistidine in a water droplet.[11] In the charged polyhistidine−water system the macroion lies entirely in the interior of the droplet. Below the Rayleigh limit the droplet shrinks in a way described by CRM. Beyond the Rayleigh limit the water molecules form spines that distribute the charge in space and evaporation of water or other ions becomes scarce. The different mechanisms arise from the location of the macroions in the droplet, which in turn is determined from the degree of hydrophilicity of the macroions. In the charged PEG−water system the mechanism has phenomenological similarities with the IEM for macroions[25,47] if one looks in Figure 9b,c. However, the simulations show that the release of the macroion is not an activated process but a drying-out process.

CONCLUSION

In this paper, we investigated the conformational transition of poly(ethylene glycol) induced by charge in a vacuum and nanodroplets via molecular simulations. Our goal was to present more unified picture of the phenomenon by examining various aspects of it using a simple but realistic polymer molecule.

Initially, we posed the question of how to establish the range of charge that we will investigate. We examined scaling of critical amount of charges Q_c with a degree of polymerization N by identifying their upper and lower bounds for N = 32, 64,128, and 256. This approach was taken to avoid the use of fractional charges on ions that might be necessary to pinpoint more accurate values of the critical charges. Rayleigh's criterion for instability of the system predicts $Q_c \propto \sqrt{N}$ and this scaling relation was found to agree well with obtained bounds for Q_c. If we do not assume $\sqrt{N}$ scaling and fit only upper bounds or lower bounds separately, we found $Q_c \propto N^{\alpha}$ where $0.41 < \alpha < 0.52$. To estimate values of charges to use in systems that are supposed to be critically charged, we chose an empirical fit $Q_c = (N/6.0)^{1/2}$.

Next, we simulated conformational transition of three PEG-$(Na^+)_n$, where n = 54, 96, 150, systems that have critical charges predicted by the empirical fit. From direct visualization the smallest system of PEG54-$(Na^+)_3$ showed frequent transition between a compact shape and a more extended shape, although the extended one did not correspond to a local minimum of the free energy profile of the system as a function of a radius of gyration. For PEG96-$(Na^+)_4$ and PEG150-$(Na^+)_5$ systems, the probability density profiles develop two and three local maxima, respectively, where compact conformations have higher probability density than extended ones. The systematic trend of higher probability density for compact conformations shows that we slightly underestimated critical charges. The bistable picture is also consistent with previous theoretical and computational studies.

Lastly, solvation effects of the charged PEG were investigated by simulating PEG96-$(Na^+)_4$ system in nanosized droplets of water. To isolate effects of ions attached to the PEG96 molecule, we simulated also a neutral PEG in the same droplet. We found that in both cases, it stays in a uniformly extended conformation. The effect of sodium ions (and possibly extra ions present) was that the neutral PEG stayed in the interior of the water droplet, while the charged PEG (with or without extra sodium ions) stayed close to the surface. The behavior of the neutral PEG could be explained by its well-known hydrophilic nature. On the other hand, for the sodiated PEG, some of its hydrophilic oxygen atoms surround sodium ions, leaving hydrophobic ethylene groups exposed unfavorably to water. As a result, the whole molecule is expected to be pushed away from the interior of the water droplet. This observation agrees with simulation results,

and therefore, we believe that it is a force field independent phenomenon.

The charged PEG emerges from the water droplet saturated with charge that gives rise to a completely open conformation. Regarding direct comparison of these computational data with experimental findings, we note that the only possible source of error in the calculations is the quality of the force field. However, we examined the behavior of sodiated PEG in water droplets using different well-established in the literature force fields and the results were consistent. A possible next step in the comparison of the force fields is one to use a high quality polarizable force field designed for these systems. With a polarizable force field, the physical behavior is expected to be the same on the basis of calculations we have performed of sodium ions in polarizable water, but the duration of the processes may be different. In relation to processes that occur in electrospray, it is interesting to find out whether the conformation of PEG in the initial solution is maintained through the droplet environment and when finally it dries out. Even though we have not looked into the conformations of sodiated PEG in bulk solution containing electrolytes, we think that in bulk water the macroion will be more compact and carry less charge than the sodiated PEG that emerges from the droplet.

AUTHOR INFORMATION

Corresponding Author

*E-mail: styliani.constas@gmail.com.

ACKNOWLEDGMENT

S.C. thanks the Discovery Grant and the Accelerator Grant for Exceptional New Opportunities (AGENO) of Natural Sciences and Engineering Research Council of Canada (NSERC) for funding this research and SHARC-Net for providing the computing facilities to perform the simulations.

REFERENCES

(1) von Helden, G.; Wyttenbach, T.; Bowers, M. T. *Science* **1995**, *267*, 1483–1485.
(2) von Helden, G.; Wyttenbach, T.; Bowers, M. T. *Int. J. Mass Spectrom. Ion Processes* **1995**, *146147*, 349–364.
(3) Mao, Y.; Ratner, M. A.; Jarrold, M. F. *J. Phys. Chem. B* **1999**, *103*, 10017–10021.
(4) Konermann, L. *J. Phys. Chem. B* **2007**, *111*, 6534–6543.
(5) Kaltashov, I. A.; Abzalimov, R. R. *J. Am. Soc. Mass Spectrom.* **2008**, *19*, 1239–1246.
(6) Hogan, C. J.; Carroll, J. A.; Rohrs, H. W.; Biswas, P.; Gross, M. L. *J. Am. Chem. Soc.* **2008**, *130*, 6926–6927.
(7) Kebarle, P.; Vererk, U. H. *Mass Spetrom. Rev.* **2009**, *28*, 898–917.
(8) Williams, E. *J. Mass Spectrom.* **1996**, *31*, 831–842.
(9) Nohmi, T.; Fenn, J. *J. Am. Chem. Soc.* **1992**, *114*, 3241–3246.
(10) de la Mora, J. F. *Anal. Chim. Acta* **2000**, *406*, 93–104.
(11) Consta, S. *J. Phys. Chem. B* **2010**, *114*, 5263–5268.
(12) Hudgins, R. R.; Woenckhaus, J.; Jarrold, M. F. *Int. J. Mass Spectrom. Ion Processes* **1997**, *165*, 497–507.
(13) Ude, S.; de la Mora, J. F.; Thomson, B. A. *J. Am. Chem. Soc.* **2004**, *126*, 12184–12190.
(14) Mao, Y.; Burin, A. L.; Ratner, M. A.; Jarrold, M. F. *J. Chem. Phys.* **2002**, *116*, 9964–9974.
(15) Arteca, G. A.; Reimann, C. T.; Tapia, O. *Chem. Phys. Lett.* **2001**, *350*, 277–285.
(16) Arteca, G. A.; Reimann, C. T.; Tapia, O. *J. Phys. Chem. B* **2001**, *105*, 4992–4998.
(17) Arteca, G. A.; Reimann, C. T.; Tapia, O. *Mass Spetrom. Rev.* **2002**, *20*, 402–422.
(18) Robinson, E. W.; Garcia, D. E.; R. D. Leib, R.; Williams, E. R. *Anal. Chem.* **2006**, *78* (7), 2190–2198.
(19) Rayleigh, Lord *Philos. Mag.* **1882**, *14*, 184.
(20) Iribarne, J.; Thomson, B. *J. Chem. Phys.* **1976**, *64*, 2287–2294.
(21) Thomson, B.; Iribarne, J. *J. Chem. Phys.* **1979**, *71*, 4451–4463.
(22) Consta, S. *J. Mol. Struct.* **2002**, *591*, 131–140.
(23) Consta, S.; Mainer, K.; Novak, W. *J. Chem. Phys.* **2003**, *119*, 10125–10132.
(24) Dole, M.; Mack, L.; Hines, R.; Mobley, R.; Ferguson, L.; Alice, M. *J. Chem. Phys.* **1968**, *49*, 2240–2249.
(25) Fenn, J. B. *J. Am. Soc. Mass Spectrom.* **1993**, *4*, 524–533.
(26) Iavarone, A. T.; Williams, E. R. *J. Am. Chem. Soc.* **2003**, *125*, 2319–2327.
(27) Felitsyn, N.; Peschke, M.; Kebarle, P. *Int. J. Mass spectrom.* **2002**, *219*, 39–62.
(28) Smith, W.; Yong, C. W.; Rodger, P. M. *Mol. Simul.* **2002**, *28*, 385–471.
(29) Smith, W.; Forester, T.; Todorov, I. T. *The DL_POLY_2.0 User Manual*; STFC Daresbury Laboratory, Warrington WA4 4AD, Cheshire, U.K., 2009.
(30) http://www.ccp5.ac.uk/DL_POLY/.
(31) Jorgensen, W. L.; Tirado-Rives, J. *J. Am. Chem. Soc.* **1988**, *110*, 1657–1666.
(32) Aqvist, J. *J. Phys. Chem.* **1990**, *94*, 8021–8024.
(33) Brendsen, H. J. C.; Postma, J. P.; van Gunsteren,W. F.; Hermans, J. In *Intermolecular Forces*; Pullman, B., Ed.; Springer: Berlin, 1981; pp 331−342.
(34) Nosé, S. *Mol. Phys.* **1984**, *52*, 255–268.
(35) Hoover, W. G. *Phys. Rev. A* **1985**, *31*, 1695–1697.
(36) Frantz, D. D.; Freeman, D. L.; Doll, J. D. *J. Chem. Phys.* **1990**, *93*, 2769–2784.
(37) Geyer, C. J. *Computing Science and Statistics Proceedings of the 23 Symposium on the Interface*; American Statistical Association: New York, 1991; p 156.
(38) Xu, H.; Berne, B. J. *J. Chem. Phys.* **1999**, *110*, 10299–10306.
(39) Duane, S.; Kennedy, A.; Pendleton, B. J.; Roweth, D. *Phys. Lett. B* **1987**, *195*, 216–222.
(40) Mehlig, B.; Heermann, D. W.; Forrest, B. M. *Phys. Rev. B* **1992**, *45* (2), 679–685.
(41) Flory, P. *Principles of polymer chemistry*; Cornell University Press: Ithaca, NY, 1983.
(42) Grassberger, P.; Hegger, R. *J. Chem. Phys.* **1995**, *102*, 6881–6899.
(43) Chaikin, P. M.; Lubensky, T. C. *Principles of condensed matter Physics*; Cambridge University Press: Cambridge, U.K., 1995.
(44) Uyaver, S.; Seidel, C. *Europhys. Lett.* **2003**, *64*, 536–542.
(45) Grosberg, A. Y.; Khokhlov, A. R. *Statistical Physics of Macromolecules*; AIP Press: Melville, NY, 1994.
(46) *Polymer Handbook*; Brandrup, J., Immergut, E. H., Grulles, E. A., Eds.; Wiley: New York, 1999; Vol. 6, p 526.
(47) Kebarle, P.; Tang, L. *Anal. Chem.* **1993**, *22*, 972–986.